Ligand Fields in Planar Platinum(II) Complexes

Adam J. Bridgeman and Malcolm Gerloch*
University Chemical Laboratories, Lensfield Road, Cambridge CB2 1EW, UK

The 'd–d' transition energies in seven platinum(II) chromophores have been carefully analysed within the cellular ligand-field model. Earlier analyses are shown to be incorrect. The study distinguishes $[PtCl_3(NH_3)]^-$ and $[PtCl_3(NMe_3)]^-$ systems from $[PtCl_3(PEt_3)]^-$, $[PtCl_3(PPh_3)]^-$ and $[PtCl_3(AsPh_3)]^-$ complexes, and from *cis*-$[PtCl_2(NH_3)_2]$ and $[PtCl_2(en)]$ (en = ethane-1,2-diamine). Parameter values are unavoidably correlated in these high-symmetry species. The nitrogen, phosphorus and arsenic ligands are all stronger σ bases than is chloride. The halides act as π bases while the phosphines and arsine act as π acids. The *trans* influence of amine, phosphine and arsine is evident in the spectra of these compounds. The continued applicability of the ligand-field method in these third-row d-block species is further attested by a successful reproduction and analysis of the intensity distribution in the spectra of $[PtCl_3(NH_3)]^-$; the intensity arises from both statically and vibronically sourced parity-mixing processes.

Seven 'd–d' transitions are resolved in the spectrum[1] of the $[PtCl_4]^{2-}$ ion. This relatively rich data base, together with the simplicity of the square-planar co-ordination and monatomic halogen ligands, have established this chromophore as an ideal challenge to a variety of theoretical models. As summarized elsewhere,[2] these have included crystal-field, ligand-field, angular-overlap and other semiempirical molecular-orbital schemes, and SCF-MO (self-consistent field molecular orbital) and Xα approaches. The central issue has been the reproduction of all experimental transition energies, taking due account of some incomplete assignment requirements derived from polarized absorption and magnetic circular dichroism (MCD) experiments, and to determine the concomitant d-orbital ordering. All reasonable orbital sequences have been proposed on the basis of these various models. The correct ordering is now surely established, predominantly from two ligand-field studies. The first of these, by Vanquickenborne and Ceulemans,[3] drew on the idea of Francke and Moncuit[4] to include within their angular overlap model (AOM) a recognition of interaction between platinum 6s and $5d_{z^2}$ orbitals. It was through this important study that the $[PtCl_3(NH_3)]^-$ ion came to share centre stage with $[PtCl_4]^{2-}$ in ligand-field studies of third-row d-block complexes. The second study to establish the consistency of the ligand-field scheme and of Vanquickenborne and Ceulemans' d-orbital ordering was that of Bridgeman and Gerloch[2] who accurately reproduced the relative intensities of nine discrete bands (from two polarizations) in the spectrum in addition to the band frequencies. It was clear from the latter analysis, however, that fits to experimental transition energies are ambiguous, such that correlations, of varying extent, between the various ligand-field parameters are defined by optimum fit to the experimental data. These uncertainties do not define poor analysis but rather inevitable artefacts of the global symmetry and d^n configuration in this and related complexes. It is most important to report such ambiguities fully so that comparisons between systems, albeit somewhat semiquantitative, can be made properly.

Zink and co-workers[5–7] have extended the work of Francke and Moncuit[4] by recording the electronic spectra of single crystals of $[PtCl_3L]^-$ with L = NMe_3, PEt_3, PPh_3 and $AsPh_3$, among others. Difficulty in growing large single crystals of these compounds obliged these workers to record spectra in unidentified crystal faces. Patterson *et al.*[8] have reported solution and some MCD spectra on the *cis* and *trans* platins $[PtCl_2(NH_3)_2]$. Both solution and single-crystal spectra of $[PtCl_2(en)]$ (en = ethane-1,2-diamine) have been recorded by Martin *et al.*[9]

The aim of the present study was initially to reinvestigate the ligand-field analyses of Zink in relation to the $[PtCl_3L]^-$ species with suitably resolved spectra, bearing in mind the unavoidable parameter correlations evident in our studies of $[MX_4]^{2-}$ (M = Pt or Pd, X = Cl or Br) to gauge the surety of any bonding conclusions that may emerge. It transpired almost immediately, however, that we cannot confirm any of the calculations of Zink and co-workers. Using their interelectron repulsion, spin–orbit coupling and ligand-field e_λ parameter values, we calculate transition energies that typically differ from those of Zink and co-workers by 1000 cm^{-1} or more. Our confidence in the veracity of our own calculations is based upon the following checks: (*a*) our CAMMAG4 program package[10] is quite general with regard to d^n configuration and molecular geometry and has been continuously cross-checked against other workers' computations for many years; (*b*) we reproduce exactly the calculations of Francke and Moncuit[4] on $[PtCl_3(NH_3)]^-$; (*c*) we also agree with those reported by Vanquickenborne and Ceulemans[3] for $[PtX_4]^{2-}$ (X = Cl or Br); and (*d*) within the accuracy of the figure, we concur with the diagram published by Liehr and Ballhausen[11] for the effects of an octahedral field plus spin–orbit coupling within the full d^8 basis.

So our goal now is to re-analyse the data for the $[PtCl_3L]^-$ series, augmented by those for the platins and $[PtCl_2(en)]$. The re-examination is especially important with regard to parameter interpretation, for Zink and co-workers failed to recognize the role of holohedral symmetry[12] in these systems and so argued for a π-bonding capacity for the amine ligand. Ligand-field analyses are frequently sharpened by a simultaneous study of the spectral intensities: such has been so for our studies[2] on $[PtCl_4]^{2-}$ and various $[CuCl_4]^{2-}$ and $CuCl_2N_2$ and $CuCl_2O_2$ chromophores.[13,14] Unfortunately, it has been impossible to perform intensity analyses on most of the foregoing platinum spectra in view of their unidentified polarizations. Appropriate single-crystal spectra have been published for $[PtCl_2(en)]$ and $[PtCl_3(NH_3)]^-$. Those[9] for $[PtCl_2(en)]$, however, show clear evidence of Pt···Pt interactions, with single-crystal spectra that differ significantly from the solution spectrum, and have not, therefore, been exploited for intensity analysis. Of the present series, only $[PtCl_3(NH_3)]^-$ provides a suitable data base for intensity analysis: this is included in the present report.

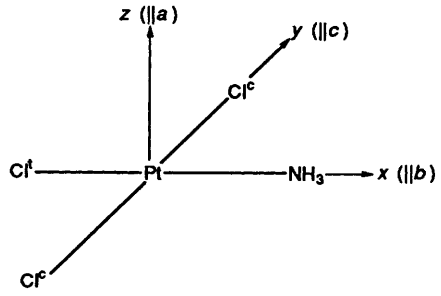

Fig. 1 Molecular axis framework and the approximate crystallographic axes (in parentheses) for the $[PtCl_3(NH_3)]^-$ ion

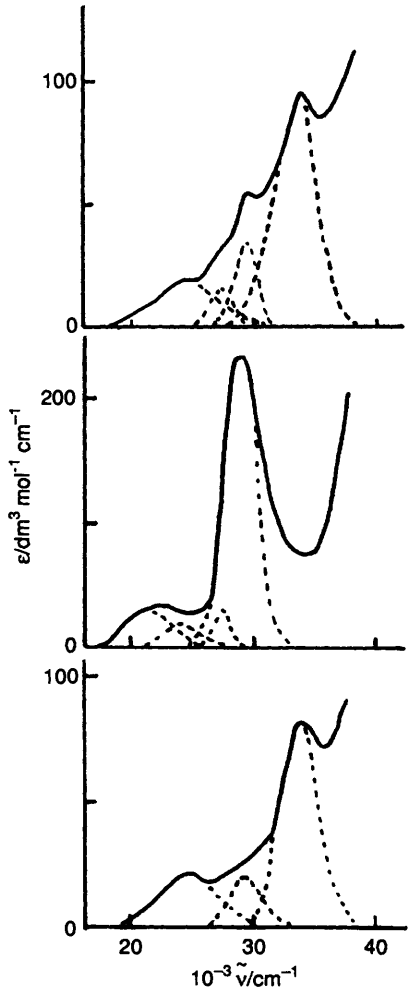

Fig. 2 Single-crystal spectra[4] at 10 K for $[PtCl_3(NH_3)]^-$ polarized along the x (upper), y (middle) and z (lower) axes. Francke and Moncuit's gaussian deconvolution is shown by the broken lines

Analyses of Transition Energies

The spectra of $[PtCl_3L]^-$ (L = NH_3, NMe_3, PEt_3, PPh_3 or $AsPh_3$) display variously better resolution than those of *cis*- and *trans*-$[PtCl_2(NH_3)_2]$ and $[PtCl_2(en)]$. Nevertheless, unacceptable degrees of ambiguity would arise in the reproduction of their transition energies in the absence of any assignment aids. As did Zink and co-workers,[5-7] therefore, we begin with $[PtCl_3(NH_3)]^-$, for which full polarization data are available, and which, together with $[PtCl_4]^{2-}$ itself, provides the key for all these analyses.

$[PtCl_3(NH_3)]^-$.—This molecule possesses near C_{2v} symmetry within an orthorhombic lattice.[15] With respect to the molecular axes labelling in Fig. 1, Fanwick and Martin[16] have

Table 1 Possible orbital transitions and selection rules for a d^8 $[PtCl_3L]^-$ complex with C_{2v} symmetry

Electronic excitation	Transition $\Gamma_1(^1A_1) \longrightarrow$	Polarization of allowed transition: Static	Vibronic
$z^2 \longrightarrow x^2 - y^2$	$^1A_1$: Γ_1	x	x, y, z
	$^3A_1$: $\Gamma_2 + \Gamma_3 + \Gamma_4$	y, z	x, y, z
$xy \longrightarrow x^2 - y^2$	$^1B_1$: Γ_2	y	x, y
	$^3B_1$: $\Gamma_1 + \Gamma_3 + \Gamma_4$	x, z	x, y, z
$yz \longrightarrow x^2 - y^2$	$^1A_2$: Γ_3	—	y, z
	$^3A_2$: $\Gamma_1 + \Gamma_2 + \Gamma_4$	x, y, z	x, y, z
$xz \longrightarrow x^2 - y^2$	$^1B_2$: Γ_4	z	x, z
	$^3B_2$: $\Gamma_1 + \Gamma_2 + \Gamma_3$	x, y	x, y, z

reported spectra at 300 and 15 K for incident light polarized parallel to y and z: fortunate alignment of the chromophore within the crystal lattice is such that $z \parallel a$, $y \parallel c$ and $x \parallel b$ very nearly. Francke and Moncuit[4] report spectra at 10 and 300 K parallel to the x, y and z molecular axes. There is broad agreement between the spectra from these two research groups, although absolute intensities differ by up to 20% on occasion. Our analyses have employed the three polarizations at 10 K of Francke and Moncuit, shown in Fig. 2.

Possible orbital transitions are labelled in Table 1, together with appropriate selection rules in C_{2v} symmetry. Following the arguments of Francke and Moncuit and of Fanwick and Martin, many of the transitions shown in Fig. 2 are assigned as follows. The band at 29 400 cm^{-1} in $c \approx y$ polarization is assigned as $\Gamma_1 \longrightarrow \Gamma_2$ ($^1A_1 \longrightarrow {}^1B_1$), and that at 33 700 cm^{-1} in $a \approx z$ polarization as $\Gamma_1 \longrightarrow \Gamma_4$ ($^1A_1 \longrightarrow {}^1B_2$). The $\Gamma_1 \longrightarrow \Gamma_3$ ($1A_1 \longrightarrow {}^1A_2$) transition is formally forbidden, a selection rule that may be violated only by small departures from molecular C_{2v} symmetry and/or dynamic contributions to intensity from vibronic coupling. The feature at *ca.* 32 500 cm^{-1} in $c \approx y$ polarization which appears as a shoulder at 300 K but vanishes at 10 K is assigned to this $\Gamma_1 \longrightarrow \Gamma_3$ transition. {We note[2] that the $\Gamma_1 \longrightarrow \Gamma_5$ (D_{4h}) transition in $[PtCl_4]^{2-}$, identified by MCD, occurs in this region and splits, $\Gamma_1 \longrightarrow \Gamma_3 + \Gamma_4$, on lowering the symmetry from D_{4h} to C_{2v}.} The $z^2 \longrightarrow x^2 - y^2$ ($\Gamma_1 \longrightarrow \Gamma_1$) transition, involving the ligand field of the co-ordination void, is expected to occur in x polarization at around 36 000 cm^{-1}. Such a band is (uniquely in the present series) observed at 38 500 cm^{-1} for $[PtCl_3(NMe_3)]^-$ by Chang and Zink.[5] Finally, bands in the region 15 000–26 000 cm^{-1} are assigned (as for the $[PtCl_4]^{2-}$ chromophore) to strongly mixed-spin transitions. The assignment requirements are all similar to those employed in the earlier analysis of the $[PtCl_4]^{2-}$ chromophore but take due account of the lower symmetry in the present series. They have been adhered to throughout our searches of parameter space throughout the ligand-field analyses reported here.

For $[PtCl_3(NH_3)]^-$, the parameter set comprises F_2 and F_4 for interelectron repulsion, ζ for spin–orbit coupling; $e_\sigma^c(Cl)$, $e_\pi^c(Cl)$ for the ligand fields of the Pt–Cl interactions normal to the Cl–Pt–NH_3 vector, $\bar{e}_\sigma$ for the mean of the diametrically opposite Pt–Cl and Pt–NH_3 ligations, $e_\pi^t(Cl)$ for the Pt–Cl π interaction opposite the Pt–NH_3 bond, and $e_\sigma(void)$ for each co-ordination void normal to the co-ordination plane. All calculations were performed, as usual, within our CAMMAG4 program suite.[10]

Good reproduction of all observed transition energies has been achieved as illustrated in Table 2. The fit is unique in kind but occurs throughout a somewhat extended region of polyparameter space. Some parameters are widely correlated, some much less so, as shown in Table 3. These ambiguities, similar to those found in our analyses of MX_4^{2-} (M = Pt or Pd,

X = Cl or Br), are inherent to these high-symmetry d^8 chromophores rather than indications of poor spectral resolution. Though unfortunate, it is appropriate that they be reported in full and that subsequent interpretations are made with due care.

$[PtCl_3(NMe_3)]^-$.—Single-crystal spectra at room temperature and 10 K have been reported by Chang and Zink [5] for an unidentified crystal face. As did these authors, we follow the assignment requirements above. As noted earlier, a band at 38 500 cm^{-1}, assigned as $\Gamma_1 \longrightarrow \Gamma_1$, is uniquely observed in the present series for this methylamine complex: it is either obscured by charge-transfer bands or lies outside the spectrometer window for the other systems.

The spectra of the amine and ammine chromophores are closely similar. Zink and co-workers note a small red shift of *ca.* 1000 cm^{-1} for the NMe_3 relative to the NH_3 complex. They also claim another difference, as follows. A weak shoulder on the band at *ca.* 32 500 cm^{-1} of the ammine complex, apparently vibronic in origin, is assigned to as $\Gamma_1 \longrightarrow \Gamma_3$. Zink and co-workers have argued that this transition is significantly shifted, to *ca.* 34 850 cm^{-1}, in the amine spectrum, their claim deriving entirely from a gaussian deconvolution of the spectral trace. After extensive searches of parameter space within the same model used for the ammine molecule, we find that no fit to all transition energies in the amine spectrum is possible unless $e_\pi^t(Cl)$ is about twice the value found for $[PtCl_3(NH_3)]^-$. We can see no reason why such a dramatic increase in this π-bonding role should accompany the replacement of NH_3 by NMe_3 in the *trans* position and have therefore discarded the possibility of the $\Gamma_1 \longrightarrow \Gamma_3$ transition at *ca.* 34 850 cm^{-1}. The close similarity of the remaining transitions, those directly observed, of the amine and ammine complexes then leaves us unable to differentiate the parameter values significantly. Small decreases in $\bar{e}_\sigma$ (or in both $\bar{e}_\sigma$ and e_σ^c) suffice to reproduce the red shift noted earlier. A typical parameter set, so adjusted, is noted at the foot of Table 4, illustrating the detailed reproduction of the experimental transition energies.

The values of $e_\sigma^c(Cl)$, $e_\pi^c(Cl)$ in Table 3 are not differentiable from $e_\sigma(Cl)$, $e_\pi(Cl)$ in the $[PtCl_4]^{2-}$ chromophore; $e_\sigma(void)$ is perhaps a little larger (numerically) in the amine- or ammine-substituted species than in the tetrachloro one. Clear differentiation, however, is evident for those cellular ligand-field (CLF) parameters relating to the nitrogen ligand. Thus $\bar{e}_\sigma$

Table 2 Comparison of observed[4] and calculated[a] transition energies (cm^{-1}) in $[PtCl_3(NH_3)]^-$

Observed	Calculated	Assignment[b]
	38 552	$\longrightarrow \Gamma_1(^1A_1)$
33 700	33 763	$\Gamma_4(^1B_2)$
32 500 (sh)	33 022	$\Gamma_3(^1A_2)$
29 400–29 200	29 444	$\Gamma_2(1B_2)$
	29 209	Γ_2
27 300?	27 417	Γ_4
	26 913	Γ_3
24 300	24 308	Γ_1
23 000	23 683	Γ_3
	23 188	Γ_1
	22 935	Γ_4
	22 012	Γ_2
20 000	20 911	Γ_3
	20 058	Γ_2
	19 930	Γ_4
	19 369	Γ_1
	0	$\Gamma_1 \longrightarrow$

[a] Using $\bar{e}_\sigma$ = 15 500 cm^{-1}, F_2 = 1080 cm^{-1}, and the correlations described in Table 3. [b] Only transitions of predominantly spin singlet–singlet character are spin-labelled.

Table 4 Comparison of observed[5] and calculated[a] transition energies (cm^{-1}) in $[PtCl_3(NMe_3)]^-$

Observed	Calculated	Assignment[b]
38 540	38 100	$\longrightarrow \Gamma_1(^1A_1)$
32 700	32 916	$\Gamma_4(^1B_2)$
	32 522	$\Gamma_3(1A_2)$
28 170	28 947	$\Gamma_2(^1B_1)$
	28 693	Γ_2
27 490	26 821	Γ_4
	26 469	Γ_3
23 330	23 767	Γ_1
	23 071	Γ_3
	22 529	Γ_4
	22 496	Γ_1
	21 343	Γ_2
19 850	20 173	Γ_3
	19 443	Γ_4
	19 398	Γ_2
	18 778	Γ_1
	0	$\Gamma_1 \longrightarrow$

[a] Using $\bar{e}_\sigma$ = 15 200 cm^{-1}, $e_\pi^t(Cl)$ = 5300 cm^{-1}, $e_\sigma^c(Cl)$ = 11 600 cm^{-1}, $e_\pi^c(Cl)$ = 2800 cm^{-1}, $e_\sigma(void)$ = −7300 cm^{-1}, F_2 = 1080 cm^{-1}, F_4 = 81 cm^{-1}, and ζ = 2600 cm^{-1}. [b] Only transitions of predominantly spin singlet–singlet character are spin-labelled.

Table 3 Parameter values (cm^{-1}) affording satisfactory reproduction of transition energies in the ligand-field spectra of $[PtCl_3(NH_3)]^-$. Ranges[a] for $[PtCl_4]^{2-}$ are included for comparison

	$[PtCl_3(NH_3)]^-$		$[PtCl_4]^{2-}$
Parameter	Correlation	Range	Correlation
$\bar{e}_\sigma$[b]		15 000–16 200	11 100–12 800
$e_\pi^t(Cl)$	$-0.4\bar{e}_\sigma$ + 11 500	5 500–5 020	
$e_\sigma^c(Cl)$	$-1.3\bar{e}_\sigma$ + 32 070	12 570–11 010	
$e_\pi^c(Cl)$	$0.25\bar{e}_\sigma$ − 1075	2 675–2 975	1 540–2 900
$e_\sigma(void)$		−7 300 ± 300[c]	−6 589 to −6 861
Σ[d]		62 840–61 160[c]	43 500–60 700[c]
F_2		1 040–1 150	660–1045
F_4	$-0.17F_2$ + 265	88–69	87–75
ζ		2 600 ± 300[c]	2 674–2 166

[a] Ref. 2. [b] $\bar{e}_\sigma = \frac{1}{2}[e_\sigma(N) + e_\sigma^t(Cl)]$ for $[PtCl_3(NH_3)]^-$, $\bar{e}_\sigma = e_\sigma^c(Cl) = e_\sigma^t(Cl)$ for $[PtCl_4]^{2-}$. [c] Values not simply correlated. [d] $\Sigma = 2\bar{e}_\sigma + 2e_\sigma^c(Cl) + 2e_\sigma(void) + 4e_\pi^c(Cl) + 2e_\pi^t(Cl)$.

Table 5 Parameter values (cm^{-1}) affording satisfactory reproduction of transition energies in the ligand-field spectra of $[PtCl_3(PEt_3)]^-$, $[PtCl_3(PPh_3)]^-$ and $[PtCl_3(AsPh_3)]^-$

	$[PtCl_3(PEt_3)]^-$		$[PtCl_3(PPh_3)]^-$		$[PtCl_3(AsPh_3)]^-$	
Parameter	Correlation	Range	Correlation	Range	Correlation	Range
$\bar{e}_\sigma$ [a]		13 500–17 000		13 000–15 400		13 500–14 700
$\bar{e}_\pi$	$-0.4\bar{e}_\sigma + 9\,050$	3 650–2 250		2 700 ± 300 [b]	$-0.5\bar{e}_\sigma + 9\,700$	2 950–2 350
$e^c_\sigma(Cl)$ [c]	$-1.5\bar{e}_\sigma + 36\,370$	16 390–11 210	$-\bar{e}_\sigma + 28\,250$	15 250–12 850	$-1.2\bar{e}_\sigma + 31\,200$	15 000–13 560
$e^c_\pi(Cl)$		2 750 ± 250 [b]	$-0.2\bar{e}_\sigma + 6\,200$	3 600–3 120	$0.33\bar{e}_\sigma - 700$	3 800–4 200
e_σ(void)		−6 250 ± 250 [b]		−7 000 ± 400 [b]		−7 000 ± 400 [b]
Σ [d]		74 380–62 420 [b]		68 240–65 080 [b]		64 900–63 220 [b]
F_2		911–1 034	$-0.05\bar{e}_\sigma + 1\,770$	1 120–1 000	$-0.1\bar{e}_\sigma + 2\,340$	990–870
F_4	$-0.125F_2 + 213$	99–58	$0.021\bar{e}_\sigma - 241$	32–82	$0.015\bar{e}_\sigma - 145$	57–76
ζ	$7.32F_2 - 4\,300$	2 400–3 300 [b]		2 900 ± 300 [b]		2 650 ± 300 [b]

[a] $\bar{e}_\sigma = \frac{1}{2}[e_\sigma(X) + e^t_\sigma(Cl)]$. [b] Values not simply correlated. [c] $\bar{e}_\pi = \frac{1}{2}[e_\pi(X) + e^t_\pi(Cl)]$. [d] $\Sigma = 2\bar{e}_\sigma + 2e^c_\sigma(Cl) + 2e_\sigma(void) + 4e^c_\pi(Cl) + 4\bar{e}_\pi$.

$\{= \frac{1}{2}[e_\sigma(N) + e_\sigma(Cl)]\}$ is some 3000–5000 cm^{-1} larger than $e_\sigma(Cl)$ in $[PtCl_4]^{2-}$; and $e^t_\pi(Cl)$ is about twice the magnitude of $e^c_\pi(Cl)$. These values attest to the better σ-donor function of NH_3 or NMe_3 than that of chlorine. The *trans* influence is evident in the relatively augmented π-donor role of the *trans* chlorine relative to the *cis*. The small red shift of the NMe_3 derivative can be reproduced by an overall increase in the sum, Σe_σ(in-plane), by 500–800 cm^{-1}; if this is ascribed to the nitrogen ligand alone, an increase of, say, 600 cm^{-1} in $e_\sigma(NMe_3)$ relative to $e_\sigma(NH_3)$ is sufficient.

$[PtCl_3L]^-$ (L = PEt_3, PPh_3 *or* $AsPh_3$).—Zink and co-workers[6,7] have again reported spectra at 10 K and room temperature for unidentified faces of single crystals of these phosphine and arsine complexes. The transition energies are similar within the group but differ significantly from those of the ammine/amine pair of complexes.

The parameter set employed in our analyses is the same as for the nitrogen species except that $e^t_\pi(Cl)$ is replaced by the average $\bar{e}_\pi \{= \frac{1}{2}[e^t_\pi(Cl) + e^t_\pi(L)]\}$ in recognition of the expected π-bonding role of the phosphines or arsine. Independent analyses have been completed for each chromophore in this group and in each case a (broad) correlated 'unique' fit to all observed transitions was obtained. Table 5 summarizes acceptable parameter ranges. Typical fits to experiment are given in Tables 6–8.

The results for the PPh_3 and $AsPh_3$ complexes are virtually indistinguishable; those for the PEt_3 complex are perhaps slightly different. Comparing the three chromophores as a group with the pair of nitrogen-donor complexes provides the following generalities. Values of $\bar{e}_\sigma$ between the groups are not differentiated; ammine, amine, phosphorus and arsine ligands are all acting as good σ donors. On the other hand, $\bar{e}_\pi$ values are some 2500 cm^{-1} less than $e^t_\pi(Cl)$ in the nitrogen-containing species, clearly reflecting a significant π-acid role of the phosphine or arsine ligands. Further $e^c_\sigma(Cl)$ and $e^c_\pi(Cl)$ values are a little greater for the phosphine and arsine species. Apparently a lesser overall π donation from the *trans* ligands, phosphine/arsine plus *trans* chlorine, is compensated by greater σ and π donation from the *cis* chlorines. If $e_\sigma(P)$ or $e_\sigma(As)$ are somewhat different from $e_\sigma(N)$ values, the breadth of the fitting within the current analyses masks the effect. Equally beyond the resolution of the current analyses is the possibility, suggested by the parameter values in Table 5, that PEt_3 is a less good acid than is PPh_3.

cis- *and* trans-$[PtCl_2(NH_3)_2]$ *and* $[PtCl_2(en)]$.—The molecular symmetries[17] of *cis*-$[PtCl_2(NH_3)_2]$ and $[PtCl_2(en)]$ are essentially C_{2v}. We employ the reference frame shown in Fig. 3 so as to parallel that used for $[PtCl_3L]^-$ systems so far as possible, yet to include recognition of the principal symmetry elements. The (empty) highest-lying orbital is now *xy* rather than $x^2 - y^2$ as in the $[PtCl_3L]^-$ species. Apart from these

Table 6 Comparison of observed[6] and calculated[a] transition energies (cm^{-1}) in $[PtCl_3(PEt_3)]^-$

Observed	Calculated	Assignment [b]
	38 641	⟶ $\Gamma_1(^1A_1)$
36 200	36 083	$\Gamma_3(^1A_2)$
35 700	35 631	$\Gamma_4(^1B_2)$
31 300	31 509	$\Gamma_2(^1B_1)$
	30 755	Γ_2
28 300	28 444	Γ_4
	28 246	Γ_3
27 600	26 494	Γ_1
24 800	25 642	Γ_1
	24 772	Γ_3
	24 690	Γ_4
22 600	23 252	Γ_2
	22 578	Γ_2
	22 357	Γ_4
	22 126	Γ_3
	21 481	Γ_1
	0	Γ_1 ⟶

[a] Using $\bar{e}_\sigma$ = 15 000 cm^{-1}, F_2 = 1000 cm^{-1}, and the correlations described in Table 5. [b] Only transitions of predominantly spin singlet–singlet character are spin-labelled.

Table 7 Comparison of observed[7] and calculated[a] transition energies (cm^{-1}) in $[PtCl_3(PPh_3)]^-$

Observed	Calculated	Assignment [b]
	39 055	⟶ $\Gamma_1(^1A_1)$
35 310	35 228	$\Gamma_4(^1B_2)$
33 400	34 241	$\Gamma_3(^1A_2)$
31 500	31 099	Γ_2
30 460	30 479	$\Gamma_2(^1B_1)$
27 040	28 509	Γ_4
	28 481	Γ_3
	26 543	Γ_1
	25 191	Γ_3
	25 020	Γ_4
	25 013	Γ_1
22 300	23 350	Γ_2
	22 405	Γ_3
	21 549	Γ_4
	21 520	Γ_2
	20 944	Γ_1
0	0	Γ_1 ⟶

[a] Using $\bar{e}_\sigma$ = 14 500 cm^{-1} and the correlations described in Table 5. [b] Only transitions of predominantly spin singlet–singlet character are spin-labelled.

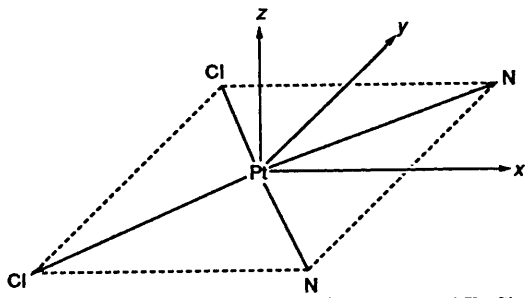

Fig. 3 Molecular axis frame for *cis*-$[PtCl_2(NH_3)_2]$ and $[PtCl_2(en)]$

Table 8 Comparison of observed[7] and calculated[a] transition energies (cm^{-1}) in $[PtCl_3(AsPh_3)]^-$

Observed	Calculated	Assignment[b]
	39 588	$\longrightarrow \Gamma_1(^1A_1)$
35 500	35 856	$\Gamma_4(^1B_2)$
33 460	34 183	$\Gamma_3(^1A_2)$
	32 130	Γ_2
29 090	29 384	$\Gamma_2(^1B_1)$
	29 204	Γ_4
	28 879	Γ_3
25 400	26 517	Γ_1
	25 347	Γ_3
	24 900	Γ_1
	24 408	Γ_4
	24 318	Γ_2
21 600	22 204	Γ_3
	21 534	Γ_2
	21 162	Γ_4
	20 698	Γ_1
	0	$\Gamma^1 \longrightarrow$

[a] Using $\bar{e}_\sigma$ = 14 100 cm^{-1} and the correlations described in Table 5. [b] Only transitions of predominantly spin singlet–singlet character are spin-labelled.

matters of definition, a physical difference arising from the change in geometry is that, within the pure d-orbital basis of the CLF modelling, holohedral symmetry establishes the *xz* and *yz* functions as degenerate.

Patterson *et al.*[8] have reported transition energies based upon solution absorption and MCD spectra. The spectra are not rich, displaying only three resolvable maxima. As before, we expect four 'singlet ⟶ singlet' transitions. However, the degeneracy of the *xz* and *yz* functions, noted above, implies that the transitions involving these orbitals are degenerate also, so reducing the number of resolvable transitions to three. Now we bear in mind the overall blue shift in the spectra expected as chlorines are replaced by the higher-field ammonia ligand: $[PtCl_4]^{2-} \longrightarrow [PtCl_3(NH_3)]^- \longrightarrow [PtCl_2(NH_3)_2]$. So the high-energy band at 38 500 cm^{-1} of $[PtCl_3(NMe_3)]^-$ is likely to lie at least as high in energy for $[PtCl_2(NH_3)_2]$, indeed beyond the range of the reported spectrum in Fig. 4. Accordingly, the two higher-energy band maxima are assigned as spin-allowed transitions. (The forbidden transition, equivalent to that in Table 1, is half of the degenerate transition just discussed and hence unresolvable experimentally.) In support of this assignment is the expectation that spin-allowed transitions in the more highly amminated complex will not fall below 26 000 cm^{-1}. The low-energy maximum in Fig. 4 is thus assigned to the various transitions of highly mixed-spin character. We have therefore considered just two assignment possibilities within our ligand-field analyses, such that the band at 35 500 cm^{-1} corresponds to the $x^2 - y^2 \longrightarrow xy$ ($\Gamma_1 \longrightarrow \Gamma_4$) transition

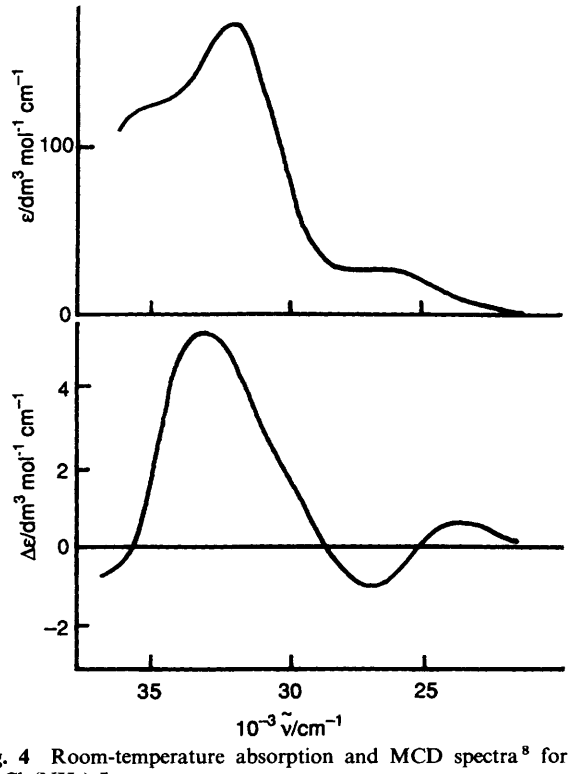

Fig. 4 Room-temperature absorption and MCD spectra[8] for *cis*-$[PtCl_2(NH_3)_2]$

with that at 32 500 cm^{-1} to the (xz, yz) ⟶ xy ($\Gamma_1 \longrightarrow \Gamma_2$, Γ_3), or *vice versa*.

The CLF parameter set comprises e_σ(void) as usual plus $\bar{e}_\sigma$ to represent the mean σ interaction of the diametrically opposite chlorine and ammonia ligations and e_π(Cl). With $\Gamma_1 \longrightarrow \Gamma_4$ assigned as the higher-energy (35 500 cm^{-1}) band, all possible agreements with all experimental transitions involve negative values for e_π(Cl). This non-physical option was discarded. Good reproduction of experiment, together with positive e_π(Cl) values, has been possible for the alternative assignment: $\Gamma_1 \longrightarrow \Gamma_2$, Γ_3 at 35 500 cm^{-1} and $\Gamma_1 \longrightarrow \Gamma_4$ at 32 500 cm^{-1} (Table 9). In view of the unfortunately poor data base offered by this spectrum, values of appropriate parameters were taken from the middle of the ranges quoted in Table 3 for the $[PtCl_3(NH_3)]^-$ chromophore, fits to experiment (shown in Table 9) being sought by variation of $\bar{e}_\sigma$ only.

Analogous procedures (see Table 10) were followed for $[PtCl_2(en)]$ the solution spectrum of which has been reported by Martin *et al.*[9] A solid-state spectrum of this complex shows evidence of significant platinum–platinum interaction which forms no part of the present investigation. The optimizations yielded $\bar{e}_\sigma$ values of 14 700 and 14 900 cm^{-1} for the diammine and ethylenediamine complexes, respectively, which are not significantly different from the 15 500 cm^{-1} (mid) value for $[PtCl_3(NH_3)]^-$. Our overall conclusion is that a good account of the 'd–d' spectral transitions in *cis*-$[PtCl_2(NH_3)_2]$ and $[PtCl_2(en)]$ is to be had with CLF parameters that are essentially the same as those appropriate in the $[PtCl_3(NH_3)]^-$ system.

Our investigations of *trans*-$[PtCl_2(NH_3)_2]$ have been unsuccessful. Patterson *et al.*[8] have reported both absorption and MCD solution spectra. Again they are not rich and one maximum in the MCD trace falls in between two, reasonably well separated, maxima in the absorption profile. Using the absorption spectrum alone, reproduction of the three observed band maxima using e_σ(N), e_σ(Cl) and e_π(Cl) together with mid-range values from the $[PtCl_3(NH_3)]^-$ analysis is possible but yields a value of $e_\sigma(NH_3)$ of *ca.* 15 000 cm^{-1}. At the same time spin-forbidden transitions are predicted to occur at *ca.* 18 000

Table 9 Comparison of observed[8] and calculated[a] transition energies (cm^{-1}) in *cis*-$[PtCl_2(NH_3)_2]$

Observed	Calculated	Assignment[b]
	40 145	$\longrightarrow \Gamma_4(^1B_2)$
35 500	36 304	$\Gamma_2(^1B_1)$
	35 932	$\Gamma_3(^1A_2)$
32 500	32 489	$\Gamma_4(^1B_2)$
30 500 (MCD)	31 162	Γ_1
	29 202	Γ_2
	29 148	Γ_3
27 000	27 293	Γ_1
	26 180	Γ_2
	26 152	Γ_3
	26 008	Γ_4
23 700 (MCD)	24 254	Γ_1
	23 463	Γ_4
	23 175	Γ_2
	23 155	Γ_3
	22 475	Γ_1
	0	$\Gamma_1 \longrightarrow$

[a] Using $\bar{e}_\sigma = 14\,700$ cm^{-1} together with the mid values from Table 3: see text. [b] Only transitions of predominantly spin singlet–singlet character are spin-labelled. Note axis framework in Fig. 3.

Table 10 Comparison of observed[9] and calculated[a] transition energies (cm^{-1}) in $[PtCl_2(en)]$

Observed	Calculated	Assignment[b]
	40 632	$\longrightarrow \Gamma_4(^1B_2)$
36 900	36 772	$\Gamma_2(^1B_1)$
	36 772	$\Gamma_3(^1A_2)$
33 200	33 236	$\Gamma_4(^1B_2)$
	31 695	Γ_1
27 300	29 739	Γ_2
	29 739	Γ_3
	28 020	Γ_1
	26 845	Γ_2
	26 845	Γ_3
	26 652	Γ_4
24 900	24 839	Γ_1
	23 990	Γ_4
	23 990	Γ_3
	23 854	Γ_2
	23 188	Γ_1
0	0	$\Gamma_1 \longrightarrow$

[a] Using $\bar{e}_\sigma = 14\,900$ cm^{-1} together with the mid values from Table 3: see text. An idealized C_{2v} molecular geometry was assumed in the analysis. [b] Only transitions of predominantly spin singlet–singlet character are spin-labelled. Note axis framework in Fig. 3.

cm^{-1}; though such bands are not observed, a rough intensity calculation {following the lines described below for the intensity analysis for $[PtCl_3(NH_3)]^-$} suggests that these transitions should have intensities about 100 times weaker than those of the observed spin-allowed features. However, the value $e_\sigma(NH_3) \approx 15\,000$ cm^{-1} does not appear to fit well with the $e_\sigma(Cl) \approx 11\,000$ cm^{-1} and $\bar{e}_\sigma\{= \frac{1}{2}[e_\sigma(N) + e_\sigma(Cl)]\} \approx 15\,000$ cm^{-1} found from the previous analyses. Other assignment choices, made in order to account for absorption and MCD spectra together, have yielded parameter values which bear no relationship whatever to those found elsewhere in this investigation. We report this unsatisfactory result merely in order to encourage a second experimental study of the spectral properties of *trans*-$[PtCl_2(NH_3)_2]$.

Analysis of the Intensity Distribution in $[PtCl_3(NH_3)]^-$

Of the eight chromophores studied here, only $[PtCl_3(NH_3)]^-$ furnishes spectra of suitable quality for intensity analysis. As noted above and in Fig. 1, the co-ordination geometry approaches C_{2v} symmetry. Our intensity analysis has employed the spectra of Francke and Moncuit,[4] shown in Fig. 2. Notwithstanding the gaussian deconvolutions performed by those workers, we have preferred to analyse only those spectral features which show reasonably clear experimental resolution. As detailed in Table 12, we seek to reproduce the relative intensities of three bands in *a* polarization, three in *b* (the middle one being the sum of the middle two in Francke and Moncuit's deconvolution), and two bands in the *c*-polarized spectrum (corresponding to the highest-energy pair and the lowest-energy pair in their gaussian deconvolution).

The chromophore is acentric.[15] Intensity is expected to arise from parity mixing within the static environment, therefore. However, the close approach of the electron density in this complex to that of its centric $[PtCl_4]^{2-}$ precursor leads one to anticipate significant contributions to the overall intensity from parity mixing arising vibronically through molecular vibrations. Our intensity analysis has therefore considered simultaneous contributions from static and vibronic sources. We have employed the same model, procedures and computing scheme as in our first such intensity analysis, for the $[Ni(en)_3]^{2+}$ cation.[18] Intensity parameters are required for the static contribution and for each normal vibrational mode of the vibronic contribution. We assume the vibronic analysis to be dominated by bending modes rather than stretches, for reasons elaborated previously.[14] The parameters for any bend are equal to those for the static contribution multiplied by the root-mean-square tangential displacement of the ligand in question; this is fully described elsewhere.[14] Tangential donor-atom displacements have been determined by normal coordinate analysis (NCA) of the vibrational frequencies of the $[PtCl_3(NH_3)]^-$ ion. Details are presented in the Appendix. Five bends have been considered for the vibronic analysis. As parameters for these are related to those for the static contribution through the NCA, as noted above, there remain just the 'static' parameters as variables within the complete intensity analysis.

Table 11 Intensity parameters[a] affording satisfactory reproduction of the relative band areas[4] in the ligand-field spectrum of $[PtCl_3(NH_3)]^-$. The analysis was predicated on the energy parameter values quoted at the foot of Table 2

Parameter	Range
${}^Pt_\sigma(N)$	110–150
${}^Ft_\sigma(N)$	0 ± 10
${}^Pt_\sigma(Cl^t)$[b]	69–123
${}^Ft_\sigma(Cl^t)$[c]	70–66
${}^Pt_\pi(Cl^t)$	0 ± 5
${}^Ft_\pi(Cl^t)$	93 ± 15
${}^Pt_\sigma(Cl^c)$	100
${}^Ft_\sigma(Cl^c)$	79 ± 15
${}^Pt_\pi(Cl^c)$	17 ± 12
${}^Ft_\pi(Cl^c)$	60 ± 5

[a] Units are D/0.015; D ≈ 3.33 × 10^{-30} C m. [b] Correlation: $1.33{}^Pt_\sigma(N) - 77$. [c] Correlation: $-0.1{}^Pt_\sigma(N) + 81$.

These variables comprise ${}^Lt_\sigma(Cl^c)$, ${}^Lt_\pi(Cl^c)$, ${}^Lt_\sigma(Cl^t)$, ${}^Lt_\pi(Cl^t)$ and ${}^Lt_\sigma(N)$, where $L = P$ or F as usual,[19] and the superscripts c and t again refer to chlorine atoms lying *cis* and *trans* to the Pt–NH_3 bond in the chromophore. From the outset, however, strong correlation between intensity parameters for the ammine and *trans*-chloro ligations were expected. Thus, insofar as total

Table 12 Band intensities for $[PtCl_3(NH_3)]^-$

(*a*) Comparison of observed[4] and calculated values*

	e ∥ *a*		*e* ∥ *b*		*e* ∥ *c*	
Band/cm^{-1}	Obs.	Calc.	Obs.	Calc.	Obs.	Calc.
18 000–25 000	51	7	42	80	72	
25 000–30 000	40	31	62	70	515	542
30 000–35 000	142	149	75	71		

(*b*) Calculated relative contributions

	e ∥ *a*		*e* ∥ *b*		*e* ∥ *c*	
Band/cm^{-1}	Static	Vibronic	Static	Vibronic	Static	Vibronic
18 000–25 000	6	1	78	2	35	5
25 000–30 000	26	5	37	33	451	91
30 000–35 000	136	13	58	23		

* Units are D^2 cm^{-1}/21.5. *e* = Electric dipole vector of the incident light.

Table A1 Wavenumbers and assignments[21] of the skeletal vibrations of the $[PtCl_3(NH_3)]^-$ ion

Vibration	Symmetry	Wavenumber*/ cm^{-1}	Approximate description
ν_1	a_1	528	Pt–N stretch
ν_2		325	Cl^1–Pt–Cl^2 symmetric stretch
ν_3		325	Pt–Cl^3 stretch
ν_4		169	In-plane Cl^1–Pt–Cl^2 bend
ν_5	b_2	169	Out-of-plane Cl^1–Pt–Cl^2 bend
ν_6		(230)	Out-of-plane N–Pt–Cl^3 bend
ν_7	b_1	324	Cl^1–Pt–Cl^2 asymmetric stretch
ν_8		(230)	Pt–N bend
ν_9		169	Pt–Cl_3 bend

* Values in parentheses are derived from combination bands.

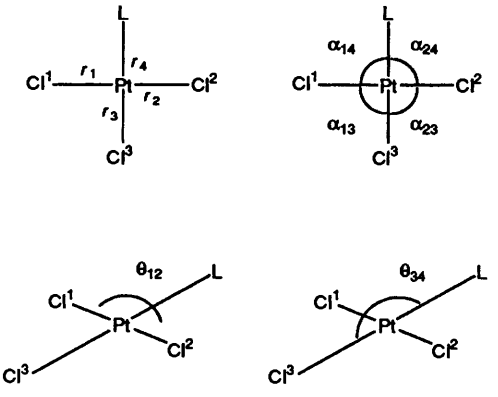

Fig. A1 Internal coordinates used in the normal coordinate analysis of the $[PtCl_3(NH_3)]^-$ ion (L = NH_3)

intensities are dominated by the static parity mixing, the difference $|^Lt_\sigma(Cl^t) - {}^Lt_\sigma(N)|$ provides the only non-vanishing source; conversely, if there were no static contribution, the electronic symmetry would be essentially centric so that no difference would exist between these two ligations. We have indeed observed this sort of parameter correlation, details being recorded in Table 11. That correlation aside, satisfactory reproduction of the intensity distribution throughout the three principal crystal polarizations has been achieved, essentially uniquely, with the parameter values given in that table. The quality of the intensity fit is shown in Table 12(*a*).

Several points arise from this unexceptional intensity analysis. It is indeed unexceptional, yielding good reproduction of the observed intensity distribution with parameter values falling within previously noted ranges.[20] The intensity arises mostly from the static parity mixing, as shown in Table 12(*b*). The more strongly bound ammine ligands are characterized by $^Pt_\sigma(N):{}^Ft_\sigma(N)$ ratios which strongly favour the *P* contribution, typical of ligand orbitals that are quite well polarized towards the metal.[20] The more equal *P* and *F* contributions of the chloride ligands are again typical of the longer, weaker halide ligations.[20] The predominance of $^Ft_\pi(Cl)$ over $^Pt_\pi(Cl)$ is also typical of earlier findings which reflect the concentration of the ligand π functions close to the donor-atom centres.[20]

Appendix

Normal Coordinate Analysis.—The nine normal modes of the $PtCl_3L$ skeleton with C_{2v} symmetry transform as $4a_1 + 3b_1 + 2b_2$ with the axes defined as above. The symmetry coordinates for this system, using the internal coordinate definitions illustrated in Fig. A1, are: a_1, $S_2 = r_4$, $S_2 = (r_1 + r_2)/2^{\frac{1}{2}}$, $S_3 = r_3$ and $S_4 = (\alpha_{14} + \alpha_{24} - \alpha_{13} - \alpha_{23})/2$; b_2, $S_5 = \theta_{12}$ and $S_6 = \theta_{34}$; b_1, $S_7 = (r_1 - r_2)/2^{\frac{1}{2}}$, $S_8 = (\alpha_{14} - \alpha_{24})/2^{\frac{1}{2}}$ and $S_9 = (\alpha_{13} - \alpha_{23})/2^{\frac{1}{2}}$. The infrared and Raman spectra of the $[PtCl_3(NH_3)]^-$ ion have been published by Denning and Ware.[21] They also report a normal coordinate analysis of a number of the observed frequencies. The infrared spectrum and a partial normal coordinate analysis has also been published by Hiraishi *et al.*[22] The assignments of the two groups differ slightly. The assignments and data of Denning and Ware, being based on polarized Raman and infrared data, are followed here. A number of the vibrations appear to be accidentally degenerate within the widths of the observed bands. The frequencies and assignments of Denning and Ware are shown in Table A1. The ammine ligand is approximated to a pseudo-monatomic unit. The calculations[23] used the crystallographically determined molecular geometry. The experimental frequencies are reproduced to within ± 1 cm^{-1} by the symmetry coordinate force constant $F_{11} = 2.55$, $F_{22} = 2.20$, $F_{33} = 1.87$, $F_{44} = 0.25$, $F_{55} = 0.25$, $F_{66} = 0.26$, $F_{77} = 1.57$, $F_{88} = 0.19$ and $F_{99} = 0.20$ (mdyn Å^{-1}) (dyn = 10^{-5} N).

Acknowledgements

A. J. B. acknowledges the receipt of an EPSRC studentship.

References

1 D. S. Martin, jun., M. A. Tucker and A. J. Kassman, *Inorg. Chem.*, 1965, **4**, 1682; 1966, **5**, 1298.

2 A. J. Bridgeman and M. Gerloch, *Mol. Phys.*, 1993, **79**, 1195.
3 L. G. Vanquickenborne and A. Ceulemans, 1981, **20**, 1981.
4 E. Francke and C. Moncuit, *Theor. Chim. Acta*, 1973, **29**, 319.
5 T.-H. Chang and J. I. Zink, *Inorg. Chem.*, 1985, **24**, 4499.
6 J. R. Phillips and J. I. Zink, *Inorg. Chem.*, 1986, **25**, 1503.
7 T.-H. Chang and J. I. Zink, *Inorg. Chem.*, 1986, **25**, 2736.
8 H. H. Patterson, J. C. Tewksbury, M. Martin, M.-B. Krogh-Jesperson, J. A. LoMenzo, H. O. Hooper and A. K. Viswanath, *Inorg. Chem.*, 1981, **20**, 2297.
9 D. S. Martin, jun., L. D. Hunter, R. Kroening and R. F. Coley, *J. Am. Chem. Soc.*, 1971, **93**, 5433.
10 CAMMAG4, a FORTRAN computer program by A. R. Dale, M. J. Duer, N. D. Fenton, M. Gerloch and R. F. McMeeking, University of Cambridge, 1991.
11 A. D. Liehr and C. J. Ballhausen, *Ann. Phys. (NY)*, 1959, **6**, 134.
12 C. K. Jørgensen, *Modern Aspects of Ligand Field Theory*, North-Holland, Amsterdam, 1971.
13 M. J. Duer, S. J. Essex and M. Gerloch, *Mol. Phys.*, 1993, **79**, 1167.
14 A. J. Bridgeman, S. J. Essex and M. Gerloch, *Inorg. Chem.*, in the press.
15 Y. P. Jeannin and D. R. Russell, *Inorg. Chem.*, 1970, **9**, 778.
16 P. E. Fanwick and D. S. Martin, jun., *Inorg. Chem.*, 1973, **12**, 24.
17 G. H. W. Milburn and M. R. Truter, *J. Chem. Soc. A*, 1966, 1610.
18 A. J. Bridgeman, M. Gerloch and K. M. Jupp, *Inorg. Chem.*, in the press.
19 C. A. Brown, M. Gerloch and R. F. McMeeking, *Mol. Phys.*, 1988, **64**, 771.
20 C. A. Brown, M. J. Duer, M. Gerloch and R. F. McMeeking, *Mol. Phys.*, 1988, **64**, 793.
21 R. G. Denning and M. J. Ware, *Spectrochim. Acta*, 1968, **24**, 1785.
22 J. Hiraishi, I. Nakagawa and T. Shimanouchi, *Spectrochim. Acta*, 1968, **24**, 1819.
23 VANAL, a FORTRAN computer program, A. J. Bridgeman and M. Gerloch, University of Cambridge, 1993.

Received 26*th August* 1994; *Paper* 4/05229C